applied sciences

MDPI

Article

A Comparative Study on the Laser Welding of Ti6Al4V Alloy Sheets in Flat and Horizontal Positions

Baohua Chang [1], Zhang Yuan [1], Haitao Pu [1], Haigang Li [2], Hao Cheng [2], Dong Du [1,*] and Jiguo Shan [1,*]

1 State Key Laboratory of Tribology, Department of Mechanical Engineering, Tsinghua University, Beijing 100084, China; bhchang@tsinghua.edu.cn (B.C.); 15201518430@163.com (Z.Y.); puhaitaohehe@163.com (H.P.)

2 Aerospace Research Institute of Materials & Processing Technology, Beijing 100076, China; lhg703@sina.com (H.L.); chenghao611@126.com (H.C.)

* Correspondence: dudong@tsinghua.edu.cn (D.D.); shanjg@tsinghua.edu.cn (J.S.); Tel.: +86-10-6278-1182 (D.D. & J.S.); Fax: +86-10-6277-3862 (D.D. & J.S.)

Academic Editor: Federico Pirzio
Received: 21 March 2017; Accepted: 6 April 2017; Published: 10 April 2017

Abstract: Laser welding has been increasingly utilized to manufacture a variety of components thanks to its high quality and speed. For components with complex shapes, the welding position needs be continuously adjusted during laser welding, which makes it necessary to know the effects of the welding position on the quality of the laser welds. In this paper, the weld quality under two (flat and horizontal) welding positions were studied comparatively in the laser welding of Ti6Al4V titanium alloy, in terms of weld profiles, process porosity, and static tensile strengths. Results show that the flat welding position led to better weld profiles, less process porosity than that of the horizontal welding position, which resulted from the different actions of gravity on the molten weld metals and the different escape routes for pores under different welding positions. Although undercuts showed no association with the fracture positions and tensile strengths of the welds, too much porosity in horizontal laser welds led to significant decreases in the strengths and specific elongations of welds. Higher laser powers and travel speeds were recommended, for both flat and horizontal welding positions, to reduce weld porosity and improve mechanical properties.

Keywords: titanium alloy; laser welding; welding position; porosity; weld profile

1. Introduction

Titanium alloys have been widely used in many industrial fields, such as aerospace and aircraft, because of their superior properties [1]. Meanwhile, lasers are applied to weld such titanium alloy components and achieve high quality at a high speed thanks to its high brightness and power availability [2]. For components with complex shapes, the weld tracks are generally not straight lines but complicated two-dimensional or three-dimensional curves (e.g., girth welds of pipelines), which lead to changes in the welding positions during laser welding. Such changes in welding positions may result in fluctuations in welding quality because of the different actions of gravity for various welding positions, which then necessitates the adjustment of welding parameters accordingly. As a basis to optimize the laser welding parameters for varying welding positions, it is therefore necessary to study the influence of welding position on weld quality.

Some research has already been done on the effects of welding position in the laser welding of steels. Guo et al. [3] indicated that employing the 2G (horizontal) welding position (with the laser beam perpendicular to the direction of gravity) could mitigate the welding defects of undercuts and sagging in laser welding of 13-mm-thickhigh strength steel plates. Such defects occurred commonly

when using the 1G (flat) welding position (with the laser beam in the same direction with gravity). Such an improvement in quality was attributed to a more balanced state for the weld pool between the surface tension, recoil pressure, and gravity. Shen et al. [4] compared the process window and porosity distribution when laser welding 10-mm-thick 30CrMnSiA ultrahigh strength steel plates using flat and horizontal positions, and found that higher line energies were required to reach the same penetration depth in the horizontal position than that for the flat position. In addition, the pores in the horizontal position laser welds were located in the upper part of the weld, while those in the flat position were in the weld center. Sohail et al. [5] studied the laser welding of 20-mm-thick low carbon steel plates in eight different welding positions, and found that the welding position had little influence on the weld bead shape and the fluid flow features of weld pools, but could lead to different levels and positions of porosity.

Besides laser welding, the effects of the welding position have also been studied for other welding processes, such as gas metal arc welding (GMAW), hybrid laser-arc welding (HLAW), and electron beam (EB) welding. Kumar and Debroy [6] numerically investigated the fluid flow during gas-metal-arc fillet welding for different various joint configurations (L and V shapes) and welding positions (tilting angles), and revealed that workpiece orientation and welding configuration could affect the free surface profile of the weld pool significantly, which might in turn affect the strength of the welds. Cho et al. [7] numerically studied the molten pool behaviors in gas metal arc welding (GMAW) of a 10-mm-thick V-groove steel plate with various welding positions (flat, overhead, and vertical). Different trends were found for humping, overflow, and lack of penetration. Lin et al. [8–10] investigated the molten pool behavior for all-position narrow gap GMAW of 25-mm-thick carbon steel plates and found that the molten pool surfaces had different shapes when welding in flat, vertical down, and overhead welding positions due to the different actions of gravity. Chen et al. [11] studied the effects of welding position on the droplet transfer behavior during hybrid CO_2 laser-MAG welding of 16-mm-thick steel and indicated that the gravity, in combination with the electromagnetic force, would cause great differences in impacting positions, modes, dimensions, and frequencies of the droplets for different welding positions (flat, horizontal, and vertical). The study by Koga et al. [12] on the all-positional electron beam welding of 19-mm-thick pipeline steel plates indicated that the optimal welding parameters were different for different welding positions, and therefore need be adjusted appropriately during a girth welding.

Existing research work on positional welding has focused mainly on thick steels used for construction of pipelines, and only a few of them are concerned with laser beam welding. Within those references, the laser welding of titanium alloy sheets under different welding positions has not been reported so far. Therefore, this research sets out to study the influence of two welding positions (flat and horizontal) on the weld quality in terms of weld profile, porosity, and strength, when laser welding Ti6Al4V titanium alloy. The results obtained can then be useful in process optimization when laser welding titanium alloy components with complex joint shapes.

2. Experimental Procedures

Titanium alloy (Ti6Al4V, annealed) sheets 3 mm in thickness were used in the study, with the chemical composition listed in Table 1. The sheets were cut into rectangular workpieces of approximately 150 mm × 300 mm. Argon with a purity of 99.998% was used as a shielding gas in all instances.

Table 1. Chemical composition of the titanium alloy Ti6Al4V sheets (wt %).

Elements	Al	V	Fe	C	N	H	O	Ti
Contents, wt %	5.8	4.0	0.2	0.05	0.03	0.011	0.19	Balance

Welding trials were performed using an IPG Photonics YLS-6000 (6 kW) Yb-fiber laser (IPG Photonics, Oxford, MS, USA) with an output wavelength of 1070 ± 10 nm. Table 2 details the collimating and

focusing units used and the resulting calculated laser beam profile characteristics. For all the trials performed, the process head was mounted on a 6-axis articulated arm robot (Reis Robotics, Obernburg, Bavaria, Germany).

Table 2. Optic combinations used in the butt welding trials.

Parameter	Value
Delivery fiber core diameter, mm	0.2
Beam parameter product, mm·mrad	6
Collimating unit focal length, mm	100
Focusing unit focal length, mm	300
Beam width, mm	0.6
Rayleigh length, mm	0.94

A schematic diagram of the laser welding setup is shown in Figure 1. Three flows of shielding gas were employed in welding. The main flow was used to protect the molten weld pool, with a rate of 20 L/min. The trailing shielding flow was used to prevent the high temperature metals that just solidified from oxidation, with a rate of 70 L/min. The root shielding flow was to protect the back surface of a specimen, with a rate of 5 L/min.

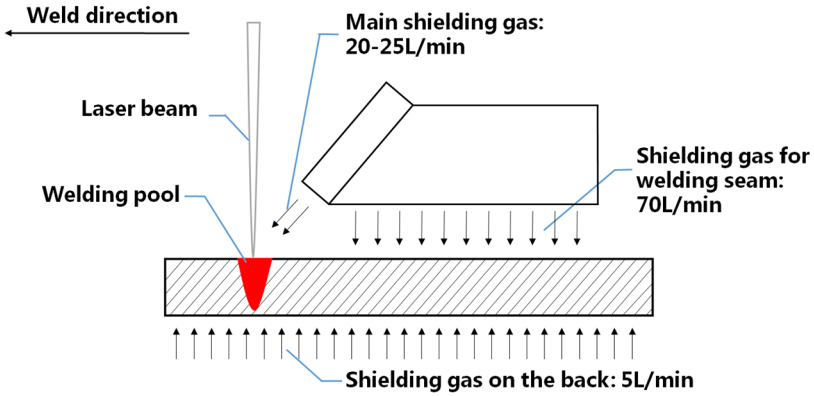

Figure 1. Schematic diagram of the laser welding setup.

The two welding positions studied (i.e., flat and horizontal) are shown in Figure 2. For each welding position, two sets of laser welding parameters were chosen, as listed in Table 3. In all welding trials, the focal position of the laser beam was located on the top surface of the workpiece.

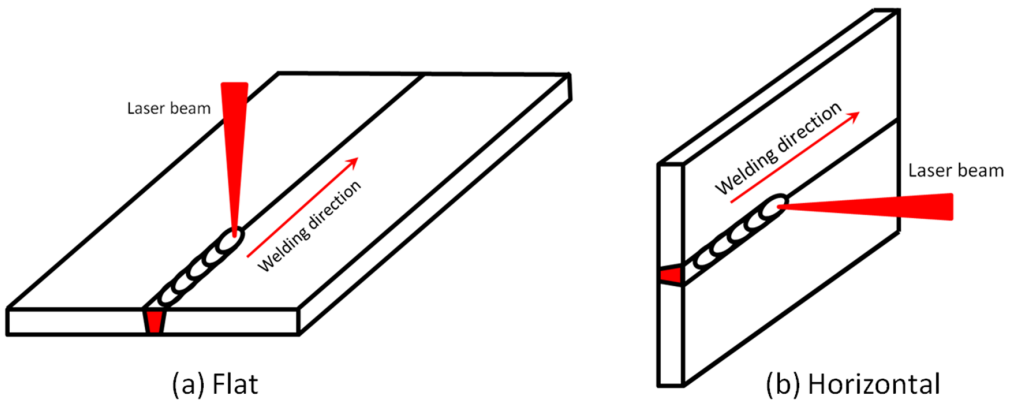

Figure 2. Two welding positions studied in the study.

Table 3. Welding parameters used in the experiments.

Welding Positions	Butt Weld Identity	Laser Power, (kW)	Welding Speed, (mm/s)	Heat Input (J/mm)
Flat	F01	2.2	8	275
	F02	2.5	20	125
Horizontal	H01	2.2	8	275
	H02	2.5	20	125

Close fitting butt welds were produced with welding conditions listed in Table 3. After welding, the specimens were firstly inspected using X-ray radiography to detect any porosity in the welds. Secondly, metallographic samples were cut from the specimen, then ground, polished and finally etched in a solution of 2 mL of HF + 10 mL of HNO_3 + 88 mL of water. The shapes and dimensions of the welds were observed and the weld profile defects were measured with an optical microscope (OM) (Olympus, Tokyo, Japan). For clarity, Figure 3 details the definition of the parameters and defects relating to weld profiles. Thirdly, static tensile tests were carried out to evaluate the mechanical properties of the welds, and fracture surfaces were examined with scanning electron microscope (SEM) (FEI Company, Hillsboro, OR, USA) to determine the fracture features. Finally, the influences of the two welding positions on the weld morphologies, porosity levels, and mechanical properties were analyzed.

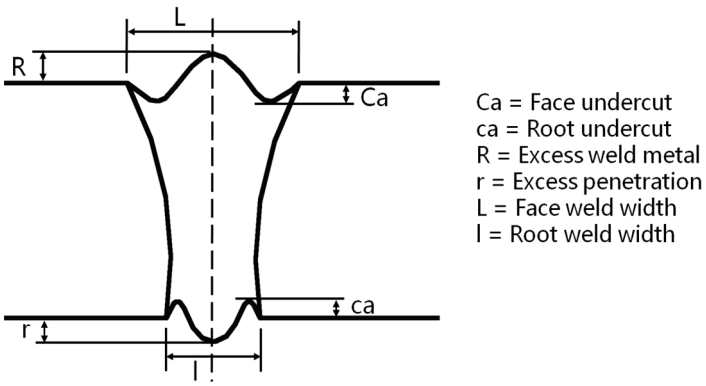

Figure 3. Weld profile parameters and defects.

3. Results

3.1. Weld Profile Defects

The cross sections of the laser welds produced with the two sets of laser welding parameters used are shown in Figures 4 and 5, respectively. The dimensions of weld profile defects measured for these laser welds are listed in Tables 4 and 5.

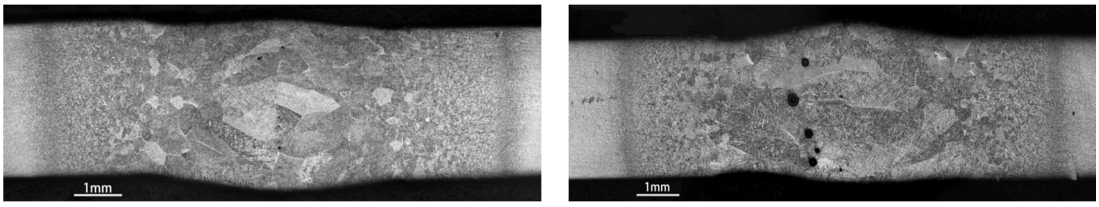

(**a**) (**b**)

Figure 4. Cross sections of laser welds (laser power: 2.2 kW; welding speed: 8 mm/s). (**a**) Flat welding; (**b**) Horizontal welding.

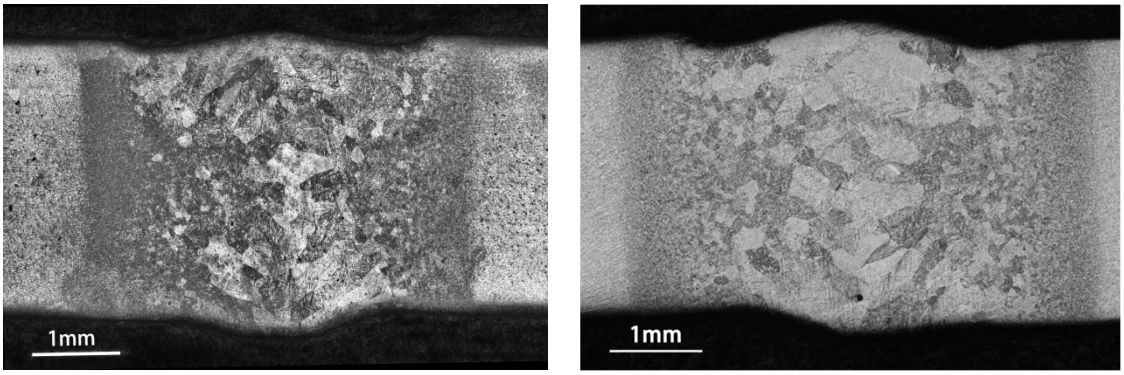

(**a**) (**b**)

Figure 5. Cross sections of laser welds (laser power: 2.5 kW; traveling speed: 20 mm/s). (**a**) Flat welding; (**b**) Horizontal welding.

Table 4. Undercuts of welds produced under different welding conditions (unit: μm).

Welding Position	Butt Weld Identity	Face Undercut		Root Undercut		Sum of Face and Root Undercuts	
		Left Side	Right Side	Left Side	Right Side	Left Side	Right Side
Flat	F01	71.1	75.8	0	0	71.1	75.8
	F02	116.1	101.9	0	23.7	116.1	125.6
Horizontal	H01	81.0	0	111.9	25.0	192.9	25
	H02	116.0	32.9	46.5	0	162.5	32.9

Table 5. Excess weld metals, excess penetrations, face and root weld widths for different welding conditions (unit: μm).

Welding Position	Butt Weld Identity	Excess Weld Metal	Excess Penetration	Face Weld Width	Root Weld Width
Flat	F01	11.8	252.4	6194.3	6111.4
	F02	86.1	314.0	3784.4	3265.4
Horizontal	H01	255.8	100.3	6546.6	6339.7
	H02	199.1	173.8	4169.0	3470.7

Table 4 lists the undercuts of welds, from which it can be found that, for flat welds, the face undercut is greater than the root undercut. Undercuts on the left side and the right side are essentially the same, i.e., symmetrical about the weld centerline. A decrease in heat input (i.e., using 2.5 kW and 20 mm/s, instead of 2.2 kW and 8 mm/s) results in a noticeable increase in face undercut, while the root undercut is less affected. For horizontal welds, the undercuts on the left side and the right side are no longer symmetrical. The left side (which is on the top side during horizontal welding) is notably larger than the right side (which is on the bottom side during welding). A decrease in the heat input results in an increase in the face undercut but decrease in the root undercut. On the whole, flat welding leads to larger face undercuts but smaller root undercuts than horizontal welding. With regard to the sum of the face and root undercuts on the same side (i.e., left side or right side), it can be found that the sum on the left side for the horizontal welds is notably larger than that on the right side, and is also larger than both the left and right side for the flat welds.

The excess weld metal and excess penetration values are presented in Table 5. Among all welds produced in this study, the flat welds have the least excess weld metals but noticeable excess penetrations. Large differences exist between the excess weld metal and the excess penetration for flat welds. The horizontal welds have larger excess metal values than excess penetration values. The differences between the excess weld metal values and the excess penetrations are smaller than the differences for the flat welds.

The face and root weld widths of welds are also given in Table 5. For both sets of welding parameters, the face and root widths for the flat welds are slightly smaller than those for the horizontal welds. Face weld widths are larger than root weld widths for both flat welds and horizontal welds. A decrease in the heat input results in decreases in both the face weld width and root weld width, as would be anticipated.

3.2. Porosity in Welds

Figure 6 shows the X-ray radiographs of four laser butt welds produced with the two different welding positions and the two different sets of welding parameters.

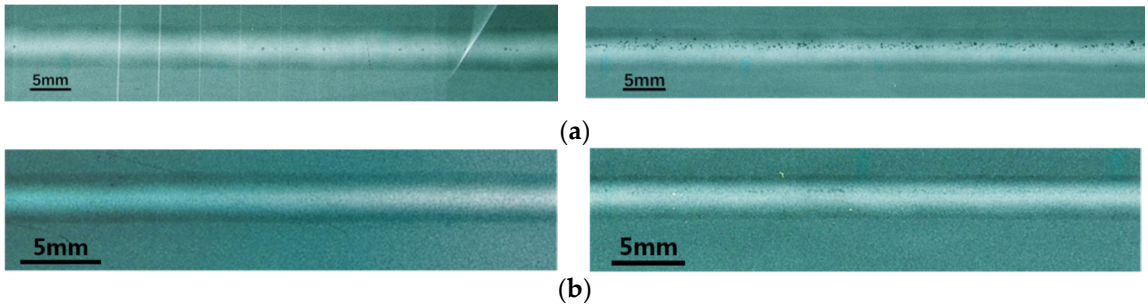

Figure 6. X-ray radiographs of butt welds made under flat and horizontal welding positions with two different sets of welding parameters. (**a**) Flat welding (**left**) versus horizontal welding (**right**) for 2.2 kW and 8 mm/s; (**b**) Flat welding (**left**) versus horizontal welding (**right**) for 2.5 kW and 20 mm/s.

For welding parameters with higher heat input (Figure 6a, heat input 275 J/mm), several isolated pores can be found along the centerline of the flat weld. By contrast, extensive chain porosity is detected above the centerline of the corresponding horizontal weld.

For welding parameters with lower heat input (Figure 6b, 125 J/mm), a limited amount of porosity can be seen in the flat weld. In the horizontal weld, fine scale chain porosity is detected. The pores are very close to each other and become indistinguishable individually, and they distribute in the upper half part of the weld.

For a quantitative characterization, the cumulative lengths of porosity over a 100 mm weld length were measured and are presented in Figure 7. It is confirmed that the porosity contents for the flat weld are lower than those in the horizontal welds. For both flat and horizontal welding positions, using higher laser power and correspondingly higher welding speed (2.5 kW, 20 mm/s) can also help to reduce the porosity content.

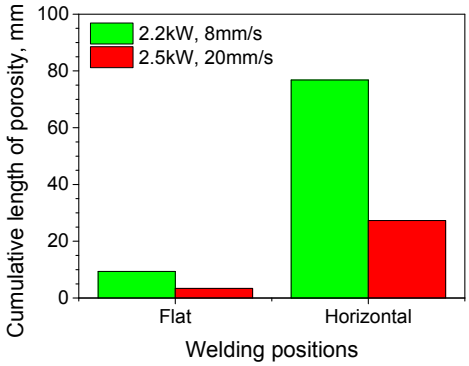

Figure 7. Cumulative lengths of porosity in welds with different welding conditions.

3.3. Mechanical Behavior

Static tensile tests showed that, irrespective of the welding position used, specimens fractured through the weld metals in welds with the lower heat input (2.5 kW and 20 mm/s), and through the base metals in welds made with higher heat input (2.2 kW and 8 mm/s).

Figure 8 shows the static tensile properties of the laser welds made using four welding conditions. It can be seen that, when a lower heat input (2.5 kW, 20 mm/s) was employed, comparable tensile strengths and specific elongations were achieved for flat welds and horizontal welds: these welds fractured through the base metals owing to the higher strengths of the weld metals compared to that of the base metal. The yield strengths of the flat welds made with the higher heat input (2.2 kW, 8 mm/s) were similar to those made with the lower heat input. By contrast, the yield strengths of the horizontal welds decreased by about 25 MPa when the higher heat input conditions were used.

In addition, marked decreases in specific elongation could be seen in both flat and horizontal welds when the higher energy input was used. Such deterioration in ductility was more significant for horizontal welds than for flat welds in these cases.

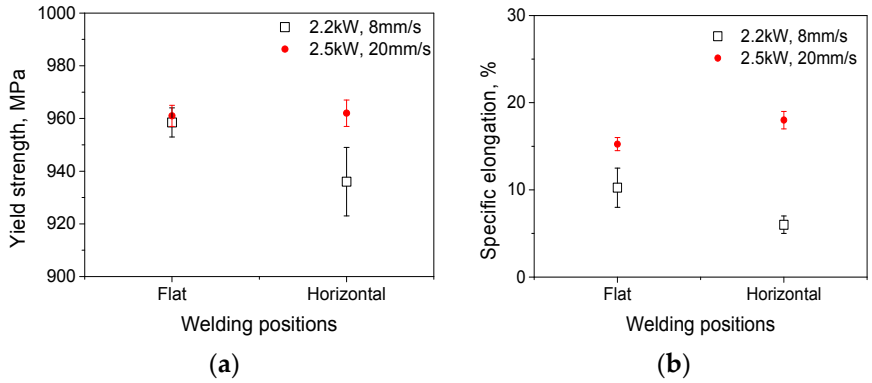

Figure 8. Static tensile properties of the laser welds made using four welding conditions. (**a**) Yield strength; (**b**) Specific elongation.

4. Discussion

4.1. Effects of Gravity on Weld Profile

Results on weld profile defects show that using the flat welding position leads to deeper undercuts on the top side than the bottom side of the weld, while using horizontal welding position leads to deeper undercuts on the left side (on the top side during welding) than on the right side (on the bottom side during welding) of the weld.

These differences can be attributed to enhanced fluid flow towards the root of the weld under the action of gravity for the flat welding position (as shown in Figure 9a); for the horizontal welding position, gravity drives the molten metal flow from the top side of the weld toward the bottom side, leading to necking on the top and thickening on the bottom (as shown in Figure 9b). Such a lateral flow also contributes to horizontal welds being wider than flat welds for a given set of welding parameters. The notable downward movement of the weld pool metal when the flat position welding also accounts for the smaller amount of excess weld metal and larger amount of excess penetration, when compared with horizontal welds.

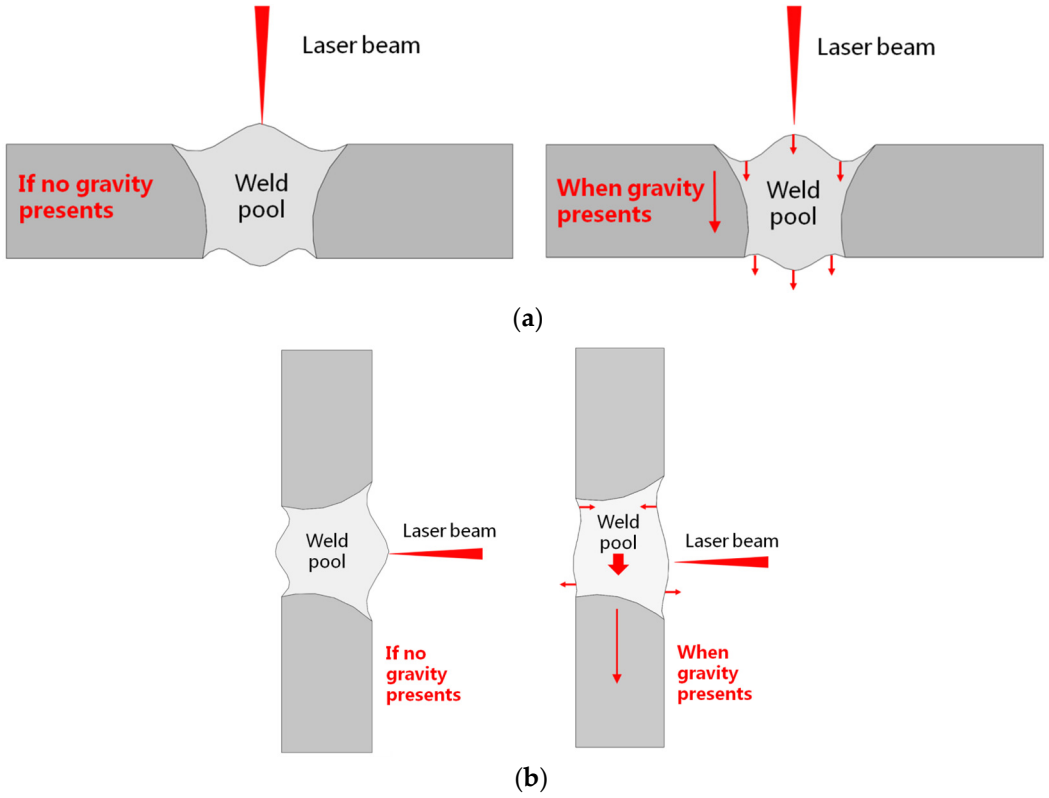

Figure 9. Schematic representation of the molten metal flow and movement of the weld pool surface due to the action of gravity in (**a**) the flat position and (**b**) the horizontal position.

4.2. Effects of Gravity on Porosity

Porosity content results indicated that using the flat welding position will result in less porosity when compared with the horizontal welding position. This can be attributed to the different degree of ease with which the pores can escape from the solidifying weld pool under different welding positions. As shown in Figure 10a, in flat welding, the pores formed in the weld pool will float upwards under the action of melt flow and buoyancy, which has been observed using an X-ray transmission imaging system by Katayama et al. [13,14]. Some pores can escape through the top surface of the weld pool before it solidifies, while others that are not able to escape will remain in the welds and form porosity. For horizontal welding, shown in Figure 10b, the pores formed also float upwards and move away from the weld centerline. However, the uppermost surface of the weld pool is now in contact with the unmelted base rather than free space. This restricts those pores from escaping; consequently, almost all end up entrapped within the weld bead. Therefore, a high porosity content, located above the weld centerline, exists within the horizontal welds, as revealed in Figure 6, which is also visible from the cross section of the horizontal weld shown in Figure 4b.

Furthermore, the final amount of porosity in a weld, especially when horizontal welding, will depend on the amount of pores formed during welding, which is closely related to the stability of the keyhole and the fluid flow characteristics in the weld pool. Results (Figure 6) show that higher power (2.5 kW) at higher welding speed (20 mm/s) result in less porosity compared with lower power (2.2 kW) at lower speed (8 mm/s). This agrees with results reported previously [15], which indicated through computational fluid dynamic (CFD) modeling that the fluid flow behind the keyhole can be quite unstable, and vortices and pores can form, particularly more so when using lower power and lower welding speed conditions. In contrast, when using higher power and welding speed conditions, CFD modelling predicted that the fluid flow would be less unstable, and fewer pores would result.

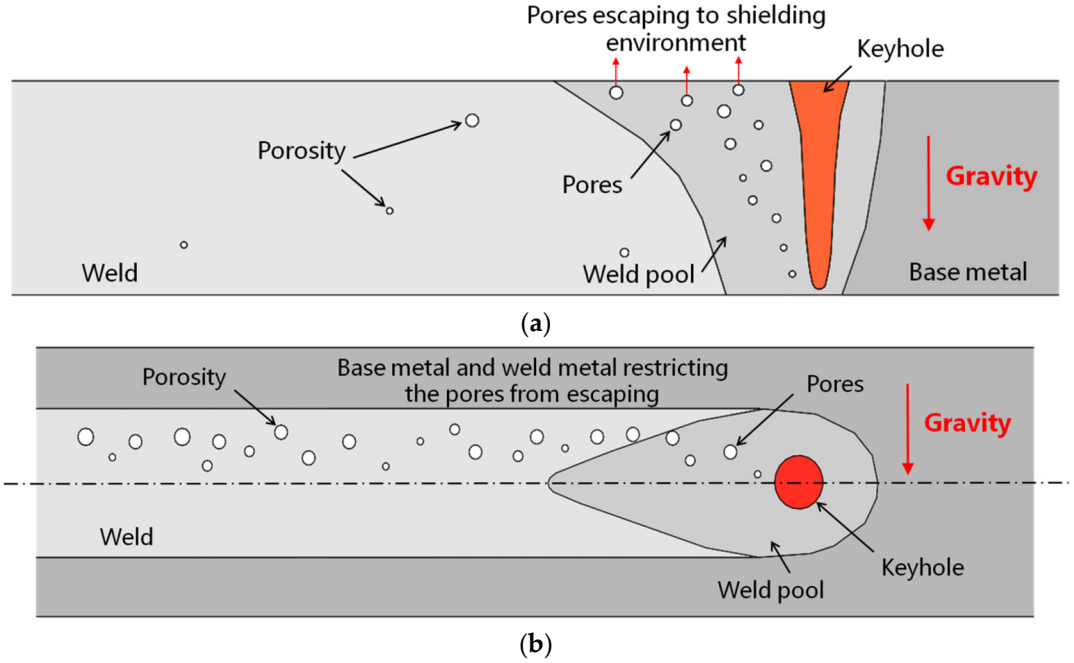

Figure 10. Schematic diagrams showing the movement of pores for (**a**) the flat position and (**b**) the horizontal position welding.

4.3. Effects of Welding Position on Static Tensile Properties

For laser welds made in Ti6Al4V, weld toe undercuts may result in high stress concentrations, which in turn lead to crack initiation and propagation during tensile testing [16]. This seems true in this work in the case of the horizontal welds made with higher heat input (2.2 kW, 8 mm/s), which had the largest undercut. However, this was not the case for the flat welds made with the same heat input, which still also fractured through the weld metal, in spite of their smaller undercuts (ref. Table 4). Evidently, the fracture position is determined not only by the degree of undercut but also other factors. It has been indicated that higher heat input will make the microstructure in the (martensitic) weld coarser, which then gives a lower toughness and a greater tendency toward cracking [16]. This could explain why all of the welds produced with a higher heat input failed through the weld metal, while those made with lower heat input failed through the base metal.

For welding conditions with higher heat input (2.2 kW, 8 mm/s), a greater amount of porosity is formed (ref. Figure 6), and this may also deteriorate weld strength. This strength deterioration is not noted in flat welds, because their porosity levels are low overall. By contrast, a great number of pores are entrapped in horizontal welds, which could then explain the notable decrease in weld strength. Figure 11 shows the comparative fractographs of a horizontal and a flat weld, both made with higher heat inputs. As Figure 11 shows, large pores are seen in the fracture face of the horizontal weld, while porosity is not detected in that of the flat weld.

Irrespective of welding position, all welds that fractured through the base metal had greater ductility than those that fractured through the weld metal. This is because the martensite of the weld metal has worse ductility than the phases (α + β) of the base metal Ti6Al4V, as previously reported [17–23]. In addition, as porosity is to the detriment of the ductility of welds when its amount reaches a certain limit [24], the great amount of porosity present in the horizontal welds could make the ductility even worse.

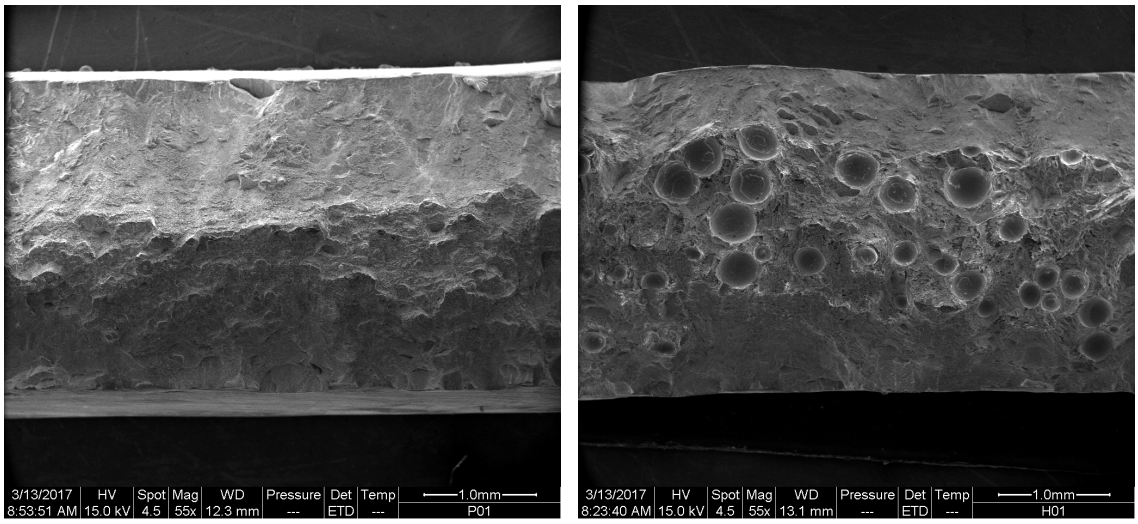

(**a**) (**b**)

Figure 11. Fractographs of the horizontal weld (**a**) and the flat weld (**b**) made with higher heat input (2.2 kW, 8 mm/s).

5. Conclusions

The following conclusions have been drawn from work carried out:

(1) For flat welds, face undercut was larger than root undercut; for horizontal welds, the undercut on the left side (top side during welding) side was larger than that on the right side (bottom side during welding).

(2) The excess penetration was greater than the excess weld metal for the flat welds, while for the horizontal welds, the excess penetration was smaller than the excess weld metal. For the same laser welding parameters, the horizontal welds were wider than the flat welds.

(3) The horizontal welding position resulted in higher weld metal porosity contents than the flat welding position, because there were fewer routes for pores to escape from the weld pool during horizontal welding. The pores were located in the center plane of the flat welds, and above the center plane of the horizontal welds.

(4) In the welds investigated, the undercuts did not show an association with the fracture positions nor the strengths in static tensile testing, although excessive porosity in laser welds did lead to significant decreases in their strength and specific elongation.

(5) Compared with a horizontal welding position, the flat welding position led to better weld formation, less porosity, and higher tensile strength. For both flat and horizontal welding positions, it is recommended to use higher laser powers and welding speeds to reduce weld porosity and improve the mechanical properties of laser welds in Ti6Al4V alloys.

Acknowledgments: This work has been financially supported by the National Natural Science Foundation of China (www.nsfc.gov.cn, No. U1537205 and No. 51675303) and the Tsinghua University Initiative Scientific Research Program (No. 2014Z05093).

Author Contributions: B.C. and D.D. conceived and designed the experiments; H.P. and H.C. performed the experiments; Z.Y. and J.S. analyzed the data; H.L. contributed reagents/materials/analysis tools; B.C. wrote the paper.

Conflicts of Interest: The authors declare no conflict of interest.

References

1. Leyens, C.; Peters, M. *Titanium and Titanium Alloys*; WILEY-VCH Verlag GmbH & Co. KGaA: Weinheim, Germany, 2003.
2. Chang, B.; Blackburn, J.; Allen, C.; Hilton, P. Studies on the spatter behaviour when welding AA5083 with a Yb-fibre laser. *Int. J. Adv. Manuf. Technol.* **2016**, *84*, 1769–1776. [CrossRef]
3. Guo, W.; Liu, Q.; Francis, J.A.; Crowther, D.; Thompson, A.; Liu, Z. Comparison of laser welds in thick section S700 high-strength steel manufactured in flat (1G) and horizontal (2G) positions. *CIRP Ann. Manuf. Technol.* **2015**, *64*, 197–200. [CrossRef]
4. Shen, X.; Li, L.; Guo, W.; Teng, W.; He, W. Comparison of processing window and porosity distribution in laser welding of 10 mm thick 30CrMnSiA ultrahigh strength between flat (1G) and horizontal (2G) positions. *J. Laser Appl.* **2016**, *28*. [CrossRef]
5. Sohail, M.; Han, S.-W.; Na, S.-J.; Gumenyuk, A.; Rethmeier, M. Numerical investigation of energy input characteristics for high-power fiber laser welding at different positions. *Int. J. Adv. Manuf. Technol.* **2015**, *80*, 931–946. [CrossRef]
6. Kumar, A.; Debroy, T. Heat transfer and fluid flow during gas-metal-arc fillet welding for various joint configurations and welding positions. *Metall. Mater. Trans. A* **2007**, *38*, 506–519. [CrossRef]
7. Cho, D.W.; Na, S.J.; Cho, M.H.; Lee, J.S. A study on V-groove GMAW for various welding positions. *J. Mater. Process. Technol.* **2013**, *213*, 1640–1652. [CrossRef]
8. Cai, X.Y.; Fan, C.L.; Lin, S.B.; Yang, C.L.; Bai, J.Y. Molten pool behaviors and weld forming characteristics of all-position tandem narrow gap GMAW. *Int. J. Adv. Manuf. Technol.* **2016**, *87*, 2437–2444. [CrossRef]
9. Xu, W.H.; Lin, S.B.; Fan, C.L.; Yang, C.L. Prediction and optimization of weld bead geometry in oscillating arc narrow gap all-position GMA welding. *Int. J. Adv. Manuf. Technol.* **2015**, *79*, 183–196. [CrossRef]
10. Xu, W.H.; Lin, S.B.; Fan, C.L.; Zhuo, X.Q.; Yang, C.L. Statistical modelling of weld bead geometry in oscillating arc narrow gap all-position GMA welding. *Int. J. Adv. Manuf. Technol.* **2014**, *72*, 1705–1716. [CrossRef]
11. Chen, Y.B.; Feng, J.C.; Li, L.Q.; Li, Y.; Chang, S. Effects of welding positions on droplet transfer in CO_2 laser-MAG hybrid welding. *Int. J. Adv. Manuf. Technol.* **2013**, *68*, 1351–1359. [CrossRef]
12. Koga, S.; Inuzuka, M.; Nagatani, H.; Iwase, T.; Masuda, H.; Ushio, M. Study of all position electron beam welding process for pipeline joints. *Sci. Technol. Weld. Join.* **2000**, *5*, 105–112. [CrossRef]
13. Katayama, S.; Mizutani, M.; Matsunawa, A. Development of porosity prevention procedures during laser welding. *Proc. SPIE* **2003**, *4831*, 281–288.
14. Katayama, S.; Seto, N.; Mizutani, M.; Matsunawa, A. Formation mechanism of porosity in high power YAG laser welding. In *Laser Materials Processing, ICALEO 2000 Proceedings*; Taylor & Francis: Abingdon, UK, 2000; Volume 89, pp. 16–25.
15. Chang, B.; Allen, C.; Blackburn, J.; Hilton, P.; Du, D. Fluid flow characteristics and porosity behavior in full penetration laser welding of a titanium alloy. *Metall. Mater. Trans B* **2015**, *46*, 906–918. [CrossRef]
16. Yang, J.; Cheng, D.; Huang, J.; Zhang, H.; Zhao, X.; Guo, H. Microstructure and mechanical properties of Ti-6AL-4V joints by laser beam welding. *Rare Metal Mater. Eng.* **2009**, *38*, 259–262. (In Chinese).
17. Mazumder, J.; Steen, W.M. Microstructure and mechanical properties of laser welded titanium 6AI-4V. *Metall. Trans. A* **1982**, *13A*, 865–871. [CrossRef]
18. Squillace, A.; Prisco, U.; Ciliberto, S.; Astarita, A. Effect of welding parameters on morphology and mechanical properties of Ti-6Al-4V laser beam welded butt joints. *J. Mater. Process. Technol.* **2012**, *212*, 427–436. [CrossRef]
19. Fang, X.; Zhang, J. Microstructural evolution and mechanical properties in laser beam welds of Ti–2Al–1.5Mn titanium alloy with transversal pre-extrusion load. *Int. J. Adv. Manuf. Technol.* **2016**, *85*, 337–343. [CrossRef]
20. Junaida, M.; Baigb, M.N.; Shamirc, M.; Khand, F.N.; Rehmana, K.; Haiderea, J. A comparative study of pulsed laser and pulsed TIG welding ofTi-5Al-2.5Sn titanium alloy sheet. *J. Mater. Process. Technol.* **2017**, *242*, 24–38. [CrossRef]
21. Hong, K.-M.; Shin, Y. C. Analysis of microstructure and mechanical properties change in laser welding of Ti6Al4V with a multiphysics prediction model. *J. Mater. Process. Technol.* **2016**, *237*, 420–429. [CrossRef]
22. Kashaev, N.; Ventzke, V.; Fomichev, V.; Fomin, F.; Riekehr, S. Effect of Nd:YAG laser beam welding on weld morphology and mechanical properties of Ti-6Al-4V butt joints and T-joints. *Opt. Lasers Eng.* **2016**, *86*, 172–180. [CrossRef]

23. Zhang, K.; Ni, L.; Lei, Z.; Chen, Y.; Hu, X. Microstructure and tensile properties of laser welded dissimilar Ti-22Al-27Nb and TA15 joints. *Int. J. Adv. Manuf. Technol.* **2016**, *87*, 1685–1692. [CrossRef]
24. Zhang, Y.; Huo, L.; Jing, H.; Pan, R. The effects of porosities and slag inclusions on mechanical properties of welded joint. *Press. Vessels* **1996**, *13*, 34–38. (In Chinese).